Materials Today Energy 7 (2018) 136–140

Contents lists available at ScienceDirect

Materials Today Energy

journal homepage: www.journals.elsevier.com/materials-today-energy/

Ab initio study of two-dimensional PdPS as an ideal light harvester and promising catalyst for hydrogen evolution reaction

Yalong Jiao [a], Fengxian Ma [a], Liujiang Zhou [b], Yun Hau Ng [c], John Bell [a], Sergei Tretiak [b], Aijun Du [a, *]

[a] School of Chemistry, Physics and Mechanical Engineering, Queensland University of Technology, Gardens Point Campus, Brisbane, QLD 4001, Australia
[b] Theoretical Division, Center for Nonlinear Studies and Center for Integrated Nanotechnologies, Los Alamos National Laboratory, Los Alamos, NM 87545, United States
[c] School of Chemical Engineering, The University of New South Wales (UNSW), Kensington, New South Wales 2052, Australia

ARTICLE INFO

Article history:
Received 27 November 2017
Received in revised form
12 January 2018
Accepted 12 January 2018

Keywords:
Hydrogen evolution reaction
Light harvester
Catalyst for water splitting
DFT calculations

ABSTRACT

The development of two-dimensional (2D) energy materials with high light absorption and ideal Gibbs free energy for hydrogen evolution reaction (HER) can propel us toward new technologies of efficient photoelectric conversion and clean energy production. Here our first-principles study depicts the 2D PdPS as a promising material for the photovoltaic solar cell and highly active catalyst for HER. Specifically, the calculated optical gap of PdPS monolayer is 1.65 eV, close to the ideal gap for solar cells. The PdPS monolayer shows a remarkably high absorbance in the visible light region and the exciton binding energy is estimated to be 0.55 eV. The PdPS sheet is found to possess highly active sites for HER, with the ideal value of Gibbs free energy, which is more desirable than that of Pt and MoS_2. Furthermore, we find the single-layer PdPS can be obtained experimentally by mechanical cleavage and it is dynamically stable by analysing its vibrational normal modes. Our work expands the family of 2D solar cells and the highly active HER activity of PdPS layer will place it as a promising catalyst for water splitting.

1. Introduction

Seeking two-dimensional (2D) materials as high-efficient photovoltaic (PV) solar cells and catalysts for water splitting provides attractive ways to produce the clean and sustainable energy without the depletion of fossil fuels and the emission of chemical pollutants [1–4]. In contrast to three dimensional (3D) bulks, the corresponding 2D sheets, which consist of only single or a few layers, always display more competitive optical properties such as stronger light absorption, thus stimulating great investigations with regard to ultra-thin solar cell fabrication. So far, a variety of 2D structures as light absorbers have been successfully realised, including transition-metal dichalcogenides (TMDs) such as MoS_2, Xenes like phosphorene, boron nitride (BN) [5], to name a few. However, some problems cannot be ignored. For example, BN layer has a very large gap [6], which hinders its ability for light absorption. Moreover, phosphorene is not very stable and can be easily oxidized when exposed to air [7]. Although single-layer MoS_2 possesses a relatively proper band gap, it is strongly influenced by structural defect [8], charged impurities [9], dielectric environment [10], etc. Thus, searching for new 2D platforms is paramountly crucial for the development of next-generation PV devices [11–13].

2D catalysts for water splitting have drawn a great attention in recent years due to their extraordinary properties [14,15]. In this context, some promising 2D materials for H_2 production by splitting water have been revealed including MoS_2/WS_2, phosphorene, nanocarbon and g-C_3N_4 [11,16–25]. Nevertheless, the reported Gibbs free energies of those well-known catalysts are not very desirable and the HER efficiency needs to be further improved. Therefore, exploring new classes of 2D materials with an ideal Gibbs free energy (~0 eV) is of importance to achieve high efficiency HER activity.

In this work, we report the PdPS monolayer as a versatile material with promising application as a light absorber and a catalyst for water splitting. By evaluating its cleavage energy and strength, we find the PdPS monolayer is highly possible to be exfoliated mechanically. The stability of the single layer is confirmed by calculating phonon band dispersions. Importantly, PdPS mono layer has an excellent optical bandgap 1.65 eV, close to the ideal band gap

* Corresponding author.
E-mail address: aijun.du@qut.edu.au (A. Du).

https://doi.org/10.1016/j.mtener.2018.01.005
2468-6069/

for solar cells (~1.4 eV). In addition, single-layer PdPS possesses multiple active sites for HER and the calculated Gibbs free energy for Pd atom is near zero, highlighting its great potential as an excellent catalyst for HER.

2. Methods

Ab initio calculations were carried out based on density functional theory (DFT) as implemented in the VASP package [26,27]. The exchange correlation functional was treated with generalized gradient approximation (GGA) in the Perdew, Burke, and Ernzerhof (PBE) form [28]. The van der Waals interactions was incorporated through the DFT-D3 approach [29]. The electron–ion interaction was described by projector-augmented-wave method [30]. A vacuum space of approximately 17 Å was applied to avoid the interaction of neighbouring layers. For geometry optimization, the plane-wave energy cut-off was set to 500 eV and a 5 × 5 × 1 Monkhorst–Pack k-points grid [31] was adopted. The convergence threshold for residual force and energy were 0.005 eV/Å and 10^{-6}eV, respectively.

Since DFT calculations are not sufficient to produce highly reliable results for 2D materials due to the ignorance of many-body effects. The GW approximation for PdPS was employed in a single shot way (G_0W_0) to compute quasi-particle (QP) band gap which was then plotted by using the maximally localized Wannier functions [32]. In addition, GW combined with Bethe–Salpeter equation (BSE) or random phase approximation (RPA) was applied to calculate light absorbance (see the details in the Supplementary material) with or without electron–hole (e–h) interactions, as implemented in BerkeleyGW package [33,34]. To carry out the BSE calculations within Tamm-Dancoff approximation, the matrix elements of BSE Hamiltonian were first computed with a 11 × 11 × 1 k-point mesh and then interpolated on a 28 × 28 × 1 mesh in which six valence bands and four conduction bands were considered.

Under the standard condition, the HER activity includes two steps. The first step is hydrogen adsorption on the catalyst (*), and the second is releasing the product hydrogen ($1/2H_2$+*). The whole process can be described as $H^+ + e^- \rightarrow \frac{1}{2}H_2$ reaction, comprising the initial state $H^+ + e^-$, the intermediate adsorbed H*, and the product hydrogen. The Gibbs free energy for the intermediate hydrogen adsorbed catalyst ($\Delta G^0_{H^*}$) is a key descriptor [35] of the HER performance in the PdPS system. It can be written as $\Delta G^0_{H^*} = \Delta E_H + 0.270\,eV$, where ΔE_H is the differential hydrogen adsorption energy. (see more HER calculation details in the Supplementary material).

3. Results and discussions

The palladium phosphide sulfide (PdPS) material has been fabricated in bulk for many years [36] and it crystallizes in an orthorhombic configuration with the space group Pbcn (no.60). The bulk configuration [37] consists of two monolayers (or four atomic layers) and the monolayer interacts with neighbouring layers through weak van der Waals forces. Each Pd atom displays in square-planar coordination and surrounded by two phosphorus and two sulphur atoms (Fig. 1c). Both P and S atoms form zig-zag chains along y-axis, resulting in a polyanion structure. The PdPS monolayer (Fig. 1b) is composed of two “atomic layers” which are connected by P–P covalent bonds. In our calculations on PBE level, the lattice constants for the PdPS bulk (Table 1) are a = 5.685 Å, b = 5.705 Å, c = 13.316 Å, which agree well with the respective experimental results [36]. The lattice constants of a single-layer PdPS (space group P2/*c*, no. 13) are a = 5.654 Å, b = 5.695 Å, slightly smaller than those of the bulk phase.

Having identified the structural configuration of PdPS, we then evaluate the possibility of extracting the monolayer from its bulk via a mechanical exfoliation strategy (see computing details in the Supplementary material). Two parameters are employed to characterize this process. The first one is the cleavage energy E_{cl}, which is the required energy over the mechanical exfoliation process. Fig. S1a illustrates the calculated E_{cl} for PdPS is 0.82 J/m^2, which is smaller than that of experimentally realised $ReSe_2$ (1.10 J/m^2) [38,39] and relatively larger than that of graphite (0.37 J/m^2) [40]. The second parameter is the cleavage strength σ as shown in Fig. S1b. Particularly, the calculated σ for PdPS is 3.48 GPa, slightly lower than the 3.59 GPa of $ReSe_2$ and comparable with the 2.10 GPa in graphite [41]. As graphene and $ReSe_2$ monolayer have been successfully exfoliated, it is also highly feasible to realize PdPS monolayer experimentally.

Next, the dynamical stability of PdPS monolayer is evaluated by calculating the phonon band spectrum. As shown in Fig. 2, no imaginary frequency can be observed at any wave vector, confirming that the single-layer PdPS is dynamically stable. To form a freestanding nanosheet, 2D PdPS should be capable to withstand external load or its own weight. Thus, the mechanical properties was estimated by the Young's modulus (Y) and Poisson's ratio (ν) as expressed below:

$$Y_x = \frac{C_{11}C_{22} - C_{12}C_{21}}{C_{22}},\ Y_y = \frac{C_{11}C_{22} - C_{12}C_{21}}{C_{11}},\ \nu_{xy} = \frac{C_{12}}{C_{22}},\ \nu_{yx} = \frac{C_{12}}{C_{11}},$$

where C_{11}, C_{12}, C_{21} and C_{22} are the elastic modulus tensor components. We therefore obtain the value of Y and ν for single-layer PdPS, which are 128 GPa·nm and 0.19 along x-axis, and 143 GPa·nm and 0.21 along y-axis, respectively. The Young's modulus along x and y are different in values, indicating the PdPS sheet is anisotropic and the in-plane stiffness along y-axis is stronger than that along x-axis. It should be noted that here the estimated Young's modulus is higher than that of 2D black phosphorus [42] and some metals such as Copper, indicating the high mechanical strength of PdPS layer and its capability to form a freestanding nanosheet after being exfoliated.

On PBE level, the PdPS bulk shows a semiconducting behavior and the indirect gap value is 0.81 eV (Fig. S2). The VBM is along the wave vector Γ-Y, while the CBM locates at a point along the D–E line. As the thickness of PdPS is gradually deceased, the quantum confinement effect becomes increasingly significant and the band gap of the system rises, followed by the expression: $E_n = E_b + A/n^\alpha$, where E_n is the band gap for n layers, E_b is the band gap for the bulk, A and α are the fitting parameters [43]. When the thickness decreases to one layer, we find the 2D PdPS shows an increasing band gap to 1.25 eV, in which both VBM and CBM are located along X-Z line (Fig. 3a). The calculation of the projected density of state demonstrates that the d orbital from Pd is the main contribution to form the CBM and VBM of single-layer PdPS. As the PBE functional has a well-known issue of gap underestimation, we then performed the hybrid density-functional (HSE06) calculations and quasiparticle G_0W_0 approximation to evaluate more accurate the gap value. As shown in Fig. 3a, the HSE06 calculation corrects the band gap of single-layer PdPS to 2.20 eV while the overall band shapes do not change compared to the PBE results. Additionally, the G_0W_0 band gap is also 2.20 eV, which agrees well with that by HSE06 method. Furthermore, the spin–orbit coupling (SOC) effect employed in calculations (Fig. S3) only leads to a negligible difference compared with the HSE06 bands. Therefore, this effect is omitted from further discussions. To further explore the electronic properties of PdPS,

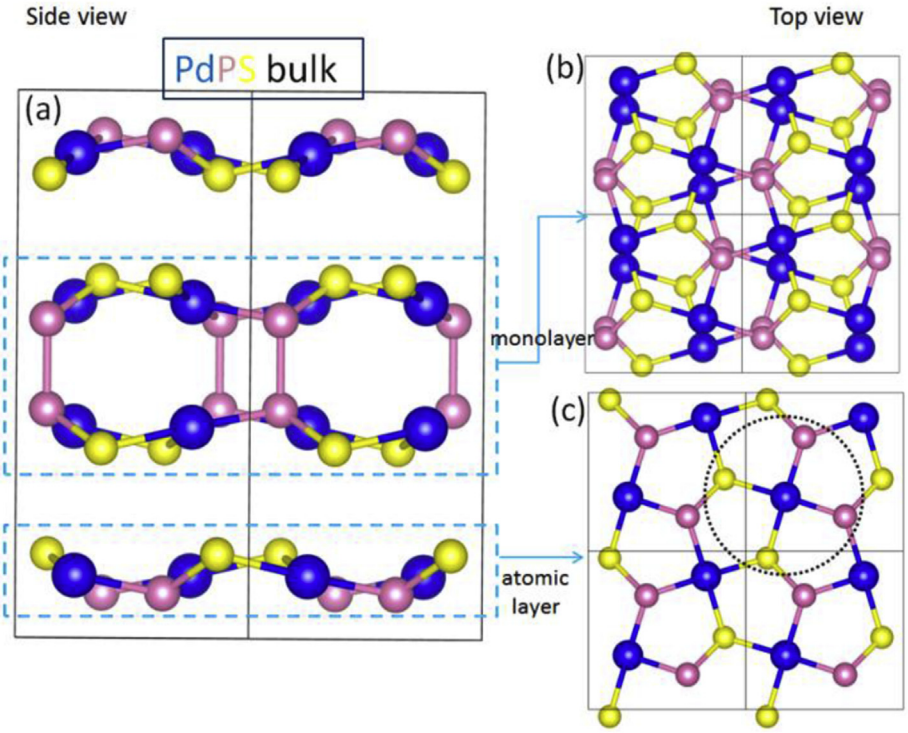

Fig. 1. (a) Side view of the PdPS bulk, (b) top view of the PdPS monolayer, (c) top view of one atomic layer PdPS. Key: blue, Pd; pink, P; yellow, S.

the band-decomposed charge density for CBM and VBM are depicted in the inset of Fig. 3b. As presented in the inset of Fig. 3b, the VBM is mainly composed by the d_{xy} orbital of Pd while the CBM is derived from the d_{z^2} orbital of Pd. In other words, the photo induced electron-hole pairs is generally attributed to the transition from the occupied d_{xy} orbital of Pd to unoccupied d_{z^2} orbital during the light harvesting process.

In addition to a PdPS monolayer, the few-layer sheet was also studied because these are easier to synthesize and common in low-dimensional material fabrication. Moreover, the electronic properties of the few-layer sheets are very fascinating according to many reports [44]. Thus, we calculated the band structures of bilayer and trilayer PdPS on the HSE06 level. We find the bilayer and trilayer PdPS are both indirect semiconductors and their gaps are 2.01 eV and 1.9 eV, respectively (Figs. S4–S5). As expected, the band gap value reduces with the rise of thickness due to the weakened quantum confinement effect as interpreted by the equation of E_n.

The band gap value and electronic band dispersion have a strong impact on the performance for light-harvesting. 2D materials usually exhibit the decreased charge screening and strengthened electron–electron (e–e) correlation, resulting in forming bound e–h pairs (excitons), which dominates the optical properties. To account for e–h interactions and yield accurate absorbance spectrum in the low-dimensional system, the GW-BSE calculation was performed and the light absorbance is shown in Fig. 4. PdPS monolayer has a QP energy gap of 2.2 eV. The first exciton peak, which corresponds to the lowest optically allowed state (optical band gap), is at 1.65 eV (Fig. 4a) and the estimated exciton binding energy is 0.55 eV. 2D PdPS shows a remarkably high absorbance in the visible light range (1.5 eV–3.0 eV). The light absorbance even hits 30% at the violet light range (around 2.9 eV). The optical gap for single-layer PdPS is smaller than that of the excellent light absorber 2D MoS_2 (1.88 eV) [45] and it is closer to the ideal gap for solar cells (~1.4 eV), indicating its great potential in photovoltaics. Moreover, the estimated exciton binding energy for single-layer PdPS is smaller than some other 2D TMDs such as MoS_2 (1.04 eV) [46], but larger than that of WS_2 (0.32 eV) [47]. Since the bandgaps of bilayer and trilayer PdPS are both smaller than that of the single layer form, it is expected that the increase of the thickness of PdPS would

Table 1
Lattice constants and volume for PdPS bulk and monolayer.

	Bulk (Cal.)	Bulk (Exp.)	Monolayer (Cal.)
a(Å)	5.685	5.677	5.654
b(Å)	5.705	5.693	5.695
c(Å)	13.316	13.304	–
v(Å)	431.934	429.974	–

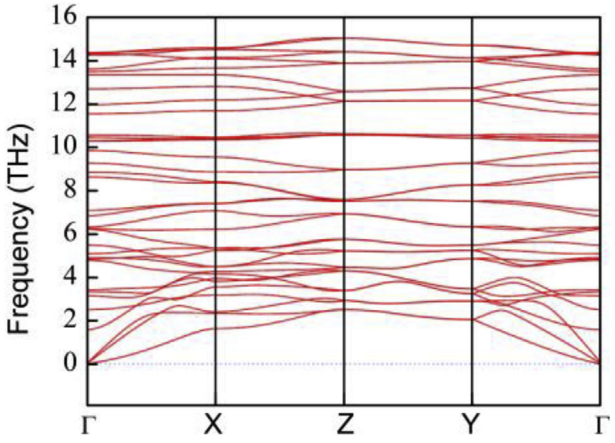

Fig. 2. Phonon dispersion of the PdPS monolayer.

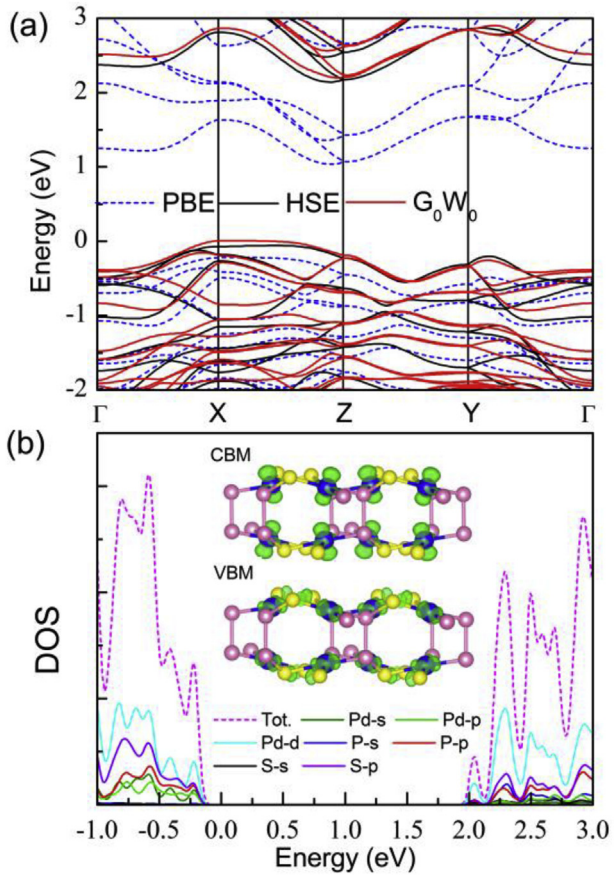

Fig. 3. (a) The band structure for PdPS monolayer calculated by PBE (dashed line), HSE06 (black solid line) and G_0W_0 (red solid line) method, respectively. (b) Density of states for PdPS monolayer calculated by HSE06 functional. Inset of (b): CBM and VBM for single-layer PdPS with an isovalue of 0.01 e/Å^3. The Fermi level is set to zero.

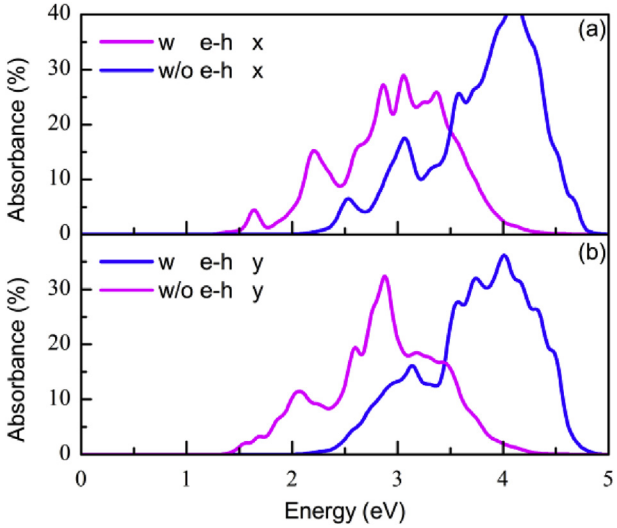

Fig. 4. Light absorbance of PdPS monolayer in the (a) x and (b) y direction, respectively. The optical absorbance without (blue) and with (pink) electron-hole interaction were obtained based on GW-RPA and GW-BSE level, respectively.

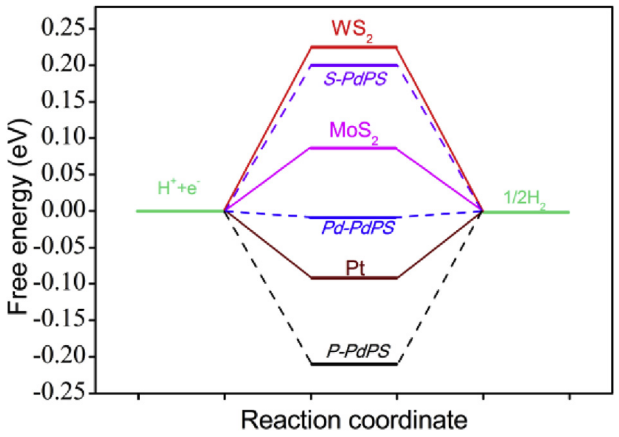

Fig. 5. The free-energy diagram of HER at different edges, i.e. Pd atom (Pd–PdPS), P atom (P–PdPS) and S atom (S–PdPS) with 1/16 hydrogen coverage, along with the referenced catalysts Pt, MoS_2, and WS_2.

redshift their absorption onset and lower the binding energy, thus broadening the solar harvesting range and enhance the ability of separating the e–h pairs, and finally increasing the efficiencies when applied in a solar cell.

In order to be an ideal catalyst for HER, the Gibbs free energy $\Delta G^0_{H^*}$ should be close to 0 [48]. A positive $\Delta G^0_{H^*}$ indicates low kinetics of hydrogen adsorption, and a negative value will lower the kinetics of hydrogen molecule release. To evaluate whether single-layer PdPS is a potential candidate for H_2 evolution, we conducted a series of theoretical investigations on edge sites. We built a 2 × 2 supercell for the single-layer PdPS which includes 16 Pd, 16 P and 16 S atoms, respectively. One H* adsorption on this layer is employed and defined as 1/16 coverage. The Pd, P and S atom are all considered as the potential adsorption sites for HER. We find the H adsorbed Pd, P and S sites are all active for HER. Specifically, H adsorbed P atom has the $\Delta G^0_{H^*}$ of −0.21 eV, while H adsorbed S site has a positive $\Delta G^0_{H^*}$ with a value of 0.20 eV. Notice that the HER performance is highly enhanced when H adsorbed on Pd atom with a $\Delta G^0_{H^*}$ of −0.01 eV (Fig. 5). This value is near-zero and slightly lower than DFT calculated value of Pt ($\Delta G^0_{H^*} \approx -0.09\,eV$) [49] or other highly active HER catalysts, e.g. MoS_2 ($\Delta G^0_{H^*} = 0.08\,eV$) and WS_2 ($\Delta G^0_{H^*} = 0.22\,eV$) [50], demonstrating the highly active HER of PdPS monolayer in terms of thermodynamics. With more active and multiple sites at the edge, the performance of PdPS catalyst is expected to be better than those of MoS_2, WS_2 and g-C_3N_4 sheets.

4. Conclusions

In conclusion, our simulations suggest that the layered 2D PdPS material is a promising 2D solar cell and an excellent catalyst for H_2 production. By calculating mechanical cleavage energy and strength, we find this sheet is feasible for experimental realisation. Moreover, the computed phonon spectrum reveals its high dynamical stability. Importantly, the optical band gap (1.65 eV) and large absorbance of PdPS suggest its potential for the photovoltaics application as a donor material. Additionally, a single layer PdPS possesses multiple active sites suitable for HER. The estimated Gibbs free energy at Pd site is close to zero and is relatively lower compared to respective values for Pt and other highly active HER catalysts including MoS_2 and WS_2, demonstrating the HER potential of PdPS monolayer. Our results highlight unique electronic and structural properties of a new 2D solar cell and catalyst for water splitting and are expected to guide future studies toward experimental realization of efficient photovoltaic applications and H_2 production based on this material.

Acknowledgment

A.D acknowledges the financial support by Australian Research Council under Discovery Project (DP170103598) and computer resources provided by NCI National Facility and The Pawsey Supercomputing Centre through the National Computational Merit Allocation Scheme supported by The Australian Government and The Government of Western Australia. L.Z and S.T acknowledge the LANL LDRD program and support of the Center for Nonlinear Studies (CNLS), the Center for Integrated Nanotechnology (CINT), a U.S. Department of Energy, Office of Basic Energy Sciences user facility.

Appendix A. Supplementary data

Supplementary data related to this article can be found at https://doi.org/10.1016/j.mtener.2018.01.005.

References

[1] K. Maeda, K. Domen, Photocatalytic water splitting: recent progress and future challenges, J. Phys. Chem. Lett. 1 (2010) 2655–2661.
[2] X. Li, Z. Li, J. Yang, Proposed photosynthesis method for producing hydrogen from dissociated water molecules using incident near-infrared light, Phys. Rev. Lett. 112 (2014) 018301.
[3] T. Zhou, Z. Cao, P. Zhang, H. Ma, Z. Gao, H. Wang, Y. Lu, J. He, Y. Zhao, Transition metal ions regulated oxygen evolution reaction performance of Ni-based hydroxides hierarchical nanoarrays, Sci. Rep. 7 (2017) 46154.
[4] M.H. Dahan, M. Caspary Toroker, Water oxidation catalysis with Fe2O3 constrained at the nanoscale, J. Phys. Chem. C 121 (2017) 6120–6125.
[5] S. Yu, X. Wu, Y. Wang, X. Guo, L. Tong, 2D materials for optical modulation: challenges and opportunities, Adv. Mater. 29 (2017).
[6] C.R. Dean, A.F. Young, I. Meric, C. Lee, L. Wang, S. Sorgenfrei, K. Watanabe, T. Taniguchi, P. Kim, K.L. Shepard, J. Hone, Boron nitride substrates for high-quality graphene electronics, Nat. Nanotechnol. 5 (2010) 722–726.
[7] A. Ziletti, A. Carvalho, D.K. Campbell, D.F. Coker, A.C. Neto, Oxygen defects in phosphorene, Phys. Rev. Lett. 114 (2015) 046801.
[8] T.S. Sreeprasad, P. Nguyen, N. Kim, V. Berry, Controlled, defect-guided, metal-nanoparticle incorporation onto MoS2 via chemical and microwave routes: electrical, thermal, and structural properties, Nano Lett. 13 (2013) 4434–4441.
[9] B. Radisavljevic, A. Kis, Mobility engineering and a metal–insulator transition in monolayer MoS2, Nat. Mater. 12 (2013) 815–820.
[10] D. Sercombe, S. Schwarz, O.D. Pozo-Zamudio, F. Liu, B.J. Robinson, E.A. Chekhovich, I.I. Tartakovskii, O. Kolosov, A.I. Tartakovskii, Optical investigation of the natural electron doping in thin MoS2 films deposited on dielectric substrates, Sci. Rep. 3 (2013).
[11] Y. Jing, Y. Ma, Y. Wang, Y. Li, T. Heine, Ultrathin layers of PdPX (X=S, Se): two dimensional semiconductors for photocatalytic water splitting, Chemistry 23 (2017) 13612–13616.
[12] Y. Jiao, F. Ma, G. Gao, J. Bell, T. Frauenheim, A. Du, Versatile single-layer sodium phosphidostannate (II): strain-tunable electronic structure, excellent mechanical flexibility, and an ideal gap for photovoltaics, J. Phys. Chem. Lett. 6 (2015) 2682–2687.
[13] F. Ma, M. Zhou, Y. Jiao, G. Gao, Y. Gu, A. Bilic, Z. Chen, A. Du, Single layer bismuth iodide: computational exploration of structural, electrical, mechanical and optical properties, Sci. Rep. 5 (2015).
[14] H.L. Zhuang, R.G. Hennig, Single-layer group-III monochalcogenide photocatalysts for water splitting, Chem. Mater. 25 (2013) 3232–3238.
[15] J. Zaffran, M.C. Toroker, Understanding the oxygen evolution reaction on a two-dimensional NiO2 catalyst, ChemElectroChem 4 (2017) 2764–2770.
[16] Y. Zheng, Y. Jiao, J. Chen, J. Liu, J. Liang, A. Du, W. Zhang, Z. Zhu, S.C. Smith, M. Jaroniec, Nanoporous graphitic-C3N4@ carbon metal-free electrocatalysts for highly efficient oxygen reduction, J. Am. Chem. Soc. 133 (2011) 20116–20119.
[17] H. Fei, J. Dong, M.J. Arellano-Jiménez, G. Ye, N.D. Kim, E.L. Samuel, Z. Peng, Z. Zhu, F. Qin, J. Bao, Atomic cobalt on nitrogen-doped graphene for hydrogen generation, Nat. Commun. 6 (2015).
[18] M.Z. Rahman, C.W. Kwong, K. Davey, S.Z. Qiao, 2D phosphorene as a water splitting photocatalyst: fundamentals to applications, Energy Environ. Sci. 9 (2016) 709–728.
[19] M.A. Lukowski, A.S. Daniel, F. Meng, A. Forticaux, L. Li, S. Jin, Enhanced hydrogen evolution catalysis from chemically exfoliated metallic MoS2 nanosheets, J. Am. Chem. Soc. 135 (2013) 10274–10277.
[20] T.F. Jaramillo, K.P. Jørgensen, J. Bonde, J.H. Nielsen, S. Horch, I. Chorkendorff, Identification of active edge sites for electrochemical H2 evolution from MoS2 nanocatalysts, Science 317 (2007) 100–102.
[21] Q. Tang, D.-e. Jiang, Mechanism of hydrogen evolution reaction on 1T-MoS2 from first principles, ACS Catal. 6 (2016) 4953–4961.
[22] G. Gao, Y. Jiao, F. Ma, Y. Jiao, E. Waclawik, A. Du, Metal-free graphitic carbon nitride as mechano-catalyst for hydrogen evolution reaction, J. Catal. 332 (2015) 149–155.
[23] K. Maeda, Photocatalytic water splitting using semiconductor particles: history and recent developments, J. Photochem. Photobiol. C Photochem. Rev. 12 (2011) 237–268.
[24] S. Sarkar, S. Sampath, Equiatomic ternary chalcogenide: PdPS and its reduced graphene oxide composite for efficient electrocatalytic hydrogen evolution, Chem. Commun. 50 (2014) 7359–7362.
[25] X. Wang, K. Maeda, A. Thomas, K. Takanabe, G. Xin, J.M. Carlsson, K. Domen, M. Antonietti, A metal-free polymeric photocatalyst for hydrogen production from water under visible light, Nat. Mater. 8 (2009) 76–80.
[26] G. Kresse, J. Furthmüller, Efficiency of ab initio total energy calculations for metals and semiconductors using a plane-wave basis set, Comput. Mater. Sci. 6 (1996) 15–50.
[27] G. Kresse, J. Furthmüller, Efficient iterative schemes for \textit{ab initio} total-energy calculations using a plane-wave basis set, Phys. Rev. B 54 (1996) 11169–11186.
[28] J.P. Perdew, K. Burke, M. Ernzerhof, Generalized gradient approximation made simple, Phys. Rev. Lett. 77 (1996) 3865–3868.
[29] S. Grimme, Semiempirical GGA-type density functional constructed with a long-range dispersion correction, J. Comput. Chem. 27 (2006) 1787–1799.
[30] P.E. Blöchl, Projector augmented-wave method, Phys. Rev. B 50 (1994) 17953–17979.
[31] H.J. Monkhorst, J.D. Pack, Special points for Brillouin-zone integrations, Phys. Rev. B 13 (1976) 5188–5192.
[32] A.A. Mostofi, J.R. Yates, Y.-S. Lee, I. Souza, D. Vanderbilt, N. Marzari, wannier90: a tool for obtaining maximally-localised Wannier functions, Comput. Phys. Commun. 178 (2008) 685–699.
[33] M. Rohlfing, S.G. Louie, Electron-hole excitations and optical spectra from first principles, Phys. Rev. B 62 (2000) 4927.
[34] J. Deslippe, G. Samsonidze, D.A. Strubbe, M. Jain, M.L. Cohen, S.G. Louie, BerkeleyGW: a massively parallel computer package for the calculation of the quasiparticle and optical properties of materials and nanostructures, Comput. Phys. Commun. 183 (2012) 1269–1289.
[35] J. Greeley, T.F. Jaramillo, J. Bonde, I. Chorkendorff, J.K. Norskov, Computational high-throughput screening of electrocatalytic materials for hydrogen evolution, Nat. Mater. 5 (2006) 909–913.
[36] T.A. Bither, P.C. Donohue, H.S. Young, Palladium and platinum phosphochalcogenides—synthesis and properties, J. Solid State Chem. 3 (1971) 300–307.
[37] J.K. Burdett, B.A. Coddens, Geometrical-electronic relationships in the series palladium diphosphide, palladium phosphide sulfide, and palladium disulfide, Inorg. Chem. 27 (1988) 418–421.
[38] D. Wolverson, S. Crampin, A.S. Kazemi, A. Ilie, S.J. Bending, Raman spectra of monolayer, few-layer, and bulk ReSe2: an anisotropic layered semiconductor, ACS Nano 8 (2014) 11154–11164.
[39] Y. Jiao, L. Zhou, F. Ma, G. Gao, L. Kou, J. Bell, S. Sanvito, A. Du, Predicting single-layer Technetium dichalcogenides (TcX2, X = S, Se) with promising applications in photovoltaics and photocatalysis, ACS Appl. Mater. Interfaces 8 (2016) 5385–5392.
[40] R. Zacharia, H. Ulbricht, T. Hertel, Interlayer cohesive energy of graphite from thermal desorption of polyaromatic hydrocarbons, Phys. Rev. B 69 (2004) 155406.
[41] S. Zhao, Z. Li, J. Yang, Obtaining two-dimensional electron gas in free space without resorting to electron doping: an electride based design, J. Am. Chem. Soc. 136 (2014) 13313–13318.
[42] J. Tao, W. Shen, S. Wu, L. Liu, Z. Feng, C. Wang, C. Hu, P. Yao, H. Zhang, W. Pang, X. Duan, J. Liu, C. Zhou, D. Zhang, Mechanical and electrical anisotropy of few-layer black phosphorus, ACS Nano 9 (2015) 11362–11370.
[43] Y. Cai, G. Zhang, Y.-W. Zhang, Layer-dependent band alignment and work function of few-layer phosphorene, Sci. Rep. 4 (2014) 6677.
[44] P.K. Das, D. Di Sante, I. Vobornik, J. Fujii, T. Okuda, E. Bruyer, A. Gyenis, B. Feldman, J. Tao, R. Ciancio, Layer-dependent quantum cooperation of electron and hole states in the anomalous semimetal WTe2, Nat. Commun. 7 (2016).
[45] D.Y. Qiu, H. Felipe, S.G. Louie, Optical spectrum of MoS 2: many-body effects and diversity of exciton states, Phys. Rev. Lett. 111 (2013) 216805.
[46] A. Ramasubramaniam, Large excitonic effects in monolayers of molybdenum and tungsten dichalcogenides, Phys. Rev. B 86 (2012) 115409.
[47] A. Chernikov, T.C. Berkelbach, H.M. Hill, A. Rigosi, Y. Li, O.B. Aslan, D.R. Reichman, M.S. Hybertsen, T.F. Heinz, Exciton binding energy and non-hydrogenic Rydberg series in monolayer WS 2, Phys. Rev. Lett. 113 (2014) 076802.
[48] Y. Jiao, Y. Zheng, M. Jaroniec, S.Z. Qiao, Design of electrocatalysts for oxygen- and hydrogen-involving energy conversion reactions, Chem. Soc. Rev. 44 (2015) 2060–2086.
[49] T. Bligaard, A. Logadottir, J. Kitchin, J. Chen, S. Pandelov, Trends in the exchange current for hydrogen evolution, J. Electrochem. Soc. 152 (2005) J23–J26.
[50] B. Hinnemann, P.G. Moses, J. Bonde, K.P. Jørgensen, J.H. Nielsen, S. Horch, I. Chorkendorff, J.K. Nørskov, Biomimetic hydrogen Evolution: MoS2 nanoparticles as catalyst for hydrogen evolution, J. Am. Chem. Soc. 127 (2005) 5308–5309.